EPJdirect A1, 1–11 (2003)
DOI 10.1007/s1010503a123

EPJdirect
electronic only

Physics Potential of ATLAS Detector with High Luminosity

Bing Zhou
(On behalf of the ATLAS Collaboration)

The University of Michigan, Ann Arbor, Michigan, USA
e-mail: bzhou@umich.edu

Received:

Abstract. The ATLAS detector is designed to exploit the full physics potential in the TeV energy region opened up by the Large Hadron Collider at a center of mass energy of 14 TeV with very high luminosities. The physics performance of the ATLAS detector on Higgs, extra-dimension and strong symmetry breaking scenario is summarized in this note. ATLAS experiment has great discovery potential for these new phenomena with high luminosity. Triple gauge couplings are very sensitive for probing new physics at TeV scale. We show that ATLAS can measure these couplings very precisely with high luminosity.

PACS: not given

1 Introduction

The Large Hadron Collider (LHC), now under construction at CERN, will collide protons at a center-of-mass energy of 14 TeV with very high luminosities of $10^{33} - 10^{34}\ cm^{-2}s^{-1}$. There is also an upgrade plan to operate the LHC with a luminosity of $10^{35}\ cm^{-2}s^{-1}$.

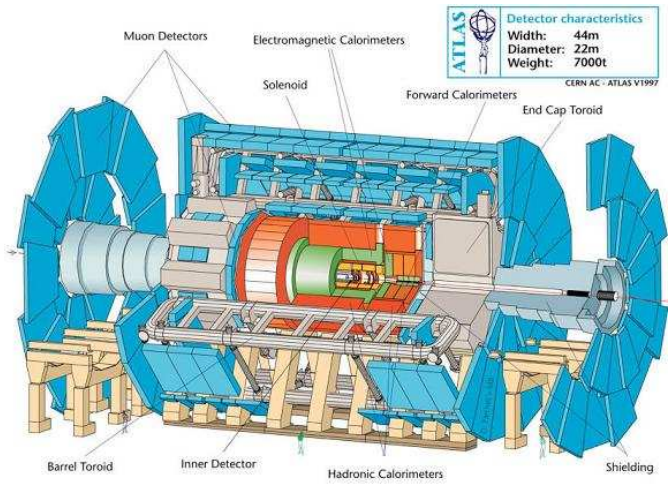

Fig. 1. *The ATLAS Detector.*

ATLAS is one of the largest and most elaborate detectors for high energy physics ever designed. Figure 1 shows an overview of the ATLAS detector, which is under construction for the first physics run in 2007. Each component of the detector is briefly summarized below:

1. **Superconducting magnets:**

a) Solenoid: provides a 2 T magnetic field for the inner detectors in a cylinder of length 6.80 m and diameter 2.30 m.

b) Barrel toroid: an air core toroid consisting of eight flat coils about the beam axis, each of length 25 m, inner diameter 9.4 m and outer diameter 20.1 m. The bending power for muon momentum measurements is typically 4 T·m.

c) Two end-cap toroids: each having eight flat coils about the beam axis. Each end-cap toroid extends for a length 5 m from the end of the barrel toroid. The end-cap toroids have inner diameter 1.65 m and outer diameter 10.7 m. They provide approximately 6 T·m bending power for muon momentum measurements in the end-cap region.

2. **Inner tracking detector:** This is contained within the solenoid, and consists of 140 million Si pixels and 6 million silicon strip detectors near the interaction point, and 0.4 million straw-tube tracking detectors with transition radiation capability in the outer part of the inner detector. The momentum resolution of the inner tracker for charged particles is $\sigma/p_T \sim 5 \times 10^{-4}\ p_T \oplus 0.001$.

3. **Electromagnetic calorimeters:** Liquid argon accordion detectors in the barrel and end-cap regions (total about 180,000 channels). The energy resolution of the electromagnetic calorimeter is $\sigma/E \sim 10\%/\sqrt{E}$.

4. **Hadronic calorimeters:** liquid argon parallel plate detectors in the end-caps ($\sim 10,000$ channels), and tile scintillators ($\sim 10,000$ channels) in the barrel region. Liquid argon tube electrode forward calorimeters extends the coverage to $\eta = 4.9$. The hadronic jet energy resolution is $\sigma/E \sim 50\%/\sqrt{E} \oplus 0.03$.

5. **Muon spectrometer:**

   a) 1194 precision tracking chambers made of 371488 monitored drift tubes (MDT) covering the tracking rapidity range of $|\eta| < 2.7$. The momentum resolution ranges from about 2% for 100 GeV muons to 10% for 1 TeV muons.

   b) 32 cathode strip chambers (CSC) consisting of 24,576 precision and 6,144 transverse coordinate strips covering the most forward rapidity region ($|\eta| = 2.0$–2.7) in the inner super-layer of the muon system.

   c) 596 resistive plate chambers (RPC) in the barrel region ($|\eta| < 1$) and 4256 thin gap chambers (TGC) in the end-cap region to provide muon triggers and to measure the second coordinate of the muon tracks.

Intensive R&D and tests on full size detector modules have shown that the ATLAS detector will have excellent lepton, photon and hadronic jet identification capabilities and accurate energy and angular measurements over almost 4π coverage.

Results presented in this paper were obtained with the full detector simulation based on GEANT3 [2] or with the ATLAS fast simulation (ATLFAST [3]), in which all responses are taken into account. Details are shown in the reference [4]. Very recently we have studied the physics potential with the upgraded luminosity of $10^{35} cm^{-2} s^{-1}$. This is summarized in reference [5].

We summarize our assumptions for integrated luminosities in different scenarios: Initial LHC luminosity ($2 \times 10^{33} cm^{-2} s^{-1}$); Standard LHC luminosity ($10^{34} cm^{-2} s^{-1}$); and Super LHC luminosity ($10^{35} cm^{-2} s^{-1}$) as shown in Table 1.

The following examples of physics discovery potential of the ATLAS experiment are presented in this paper.

- Section 2 presents the Higgs discovery signals over the entire mass range up to 1 TeV. Precision Higgs boson parameter measurements are discussed if the Higgs is discovered.

- If no Higgs is found, there will be a search for high mass resonances in longitudinal gauge boson scattering as discussed in Section 3.

Luminosity (L) ($cm^{-2}s^{-1}$)	$\int Ldt$ for one year ($10^7 sec$) of running
2×10^{33}	10 - 30 fb^{-1}
1×10^{34}	100 fb^{-1}
1×10^{35}	1000 fb^{-1}

Table 1. Luminosity scenarios of the LHC.

- Section 4 is devoted to studies of the mass reach for extra-dimension models.
- Section 5 presents the study of searches for strongly symmetry-breaking signals - technihadron resonances at the TeV scale.
- Section 6 describes precision gauge-coupling measurements to search for breakdown of the Standard Model.

2 Higgs Physics

The Standard Model (SM) of particle physics is based on two principles: gauge invariance that leads to very successful descriptions of the fundamental interactions between particles, and symmetry breaking that generates the masses for particles. A key element of the symmetry breaking in the SM is the prediction of a fundamental scalar particle, the Higgs boson, which is still waiting to be verified experimentally. The ATLAS experiment at the LHC will definitely find the Higgs boson or prove that it does not exist. This would be a big step towards understanding why particles of our universe have mass.

This section presents the ATLAS potential for discovering the SM Higgs boson in the mass range from 114 GeV, the lower limit from LEP, up to 1 TeV, the triviality bound of the theory. Measurements of Higgs parameters, such as the Higgs couplings to gauge bosons and fermions, will require high luminosities as shown in this section. Determination of Higgs self-coupling is important to understand the Higgs potential. We would have a chance to determine it at the SLHC with very high luminosities. Finally the ATLAS sensitivities to search for the MSSM Higgs bosons will be summarized.

2.1 SM Higgs Discovery Potential

The production cross-section of Higgs at the LHC is shown in Figure 2. Over the entire Higgs mass range the dominant production mechanism at the LHC is gluon fusion, and weak-boson fusion (WBF) is also important. The Higgs can also be produced associated with a vector boson, which provides an isolated lepton tag in the event, and with a top quark pair, which is an important process to measure top Yukawa coupling.

The dominant decay modes of the SM Higgs boson are W^+W^- and ZZ for a Higgs mass $M_H > 2M_Z$ and heavy fermion pairs for $M_H < 2M_Z$ as shown in Figure 3. The latter, so called low-mass region, has a very large contribution of background in two-fermion final state. Therefore, it is necessary to rely on rare decays that contain isolated energetic leptons or photons in final states. This, in fact, poses a major challenge to the design of the ATLAS detector for excellent lepton/photon identifications and energy measurements.

The goal of the ATLAS experiment is to observe clear signatures of the Higgs boson in the first year of the physics run of the LHC. We show some examples of the Higgs signature to be observed by the ATLAS experiment with 10 - 100 fb^{-1} integrated luminosity.

We first show the "gold-plated signal" from the process of $H \rightarrow ZZ \rightarrow \ell^+\ell^-\ell^+\ell^-$ ($\ell = e,\ \mu$) in Figure 4. Higgs boson can be clearly observed in four-lepton channel with an integrated luminosity of 10 fb^{-1}, when Higgs boson is heavier then $2M_Z$.

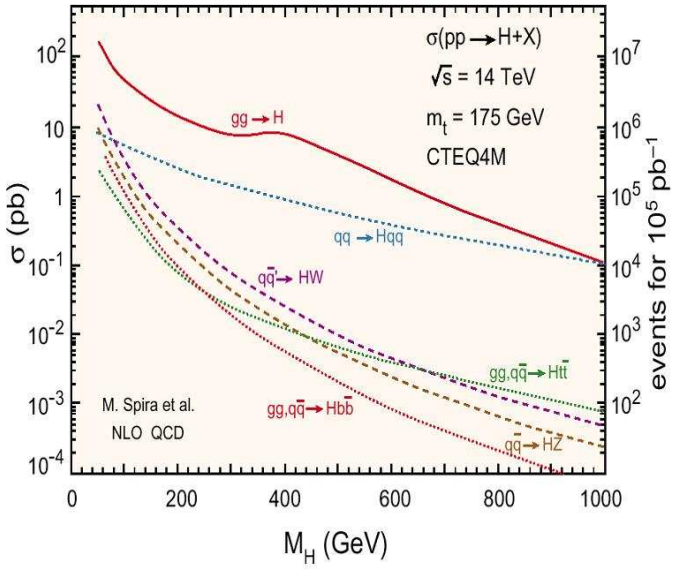

Fig. 2. *Higgs production cross sections as a function of M_H for different production mechanisms at the LHC.*

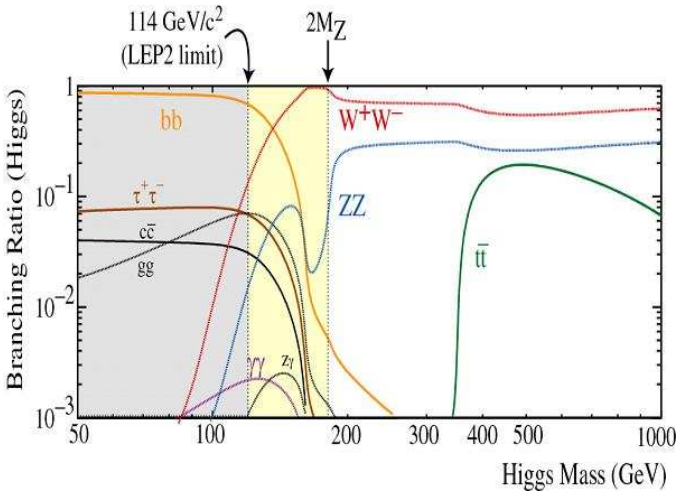

Fig. 3. *Higgs decay branching ratio as a function of M_H. The mass region between the LEP limit (114 GeV) to $2M_Z$ will be the most challenging region to discover the Higgs signals since the pure leptonic and photonic final states have very small branching ratios.*

The Higgs discovery criterion is determined by the so-called "5σ signal significance" in observations, which is defined as

$$S/\sqrt{B} \geq 5$$

where S is the observed number of signal events and B is the expected number of background events.

Higher luminosities are required to reach 5σ signal significance for light Higgs boson discovery in individual decay modes. It is important to observe various decay modes of Higgs boson since these observations will allow high precision measurements of the Higgs parameters to study the SM Higgs sector in-depth. For this purpose, a run with high luminosity is necessary.

Figure 5 shows the required integrated luminosities for low-mass Higgs discoveries [6] with the ATLAS precision Muon Spectrometer operating in a stand-alone mode[7]. The plot indicates that the low mass Higgs (130 GeV $<$ M_H $<$170 GeV) could be discovered with integrated luminosities between 12 - 80 fb^{-1}

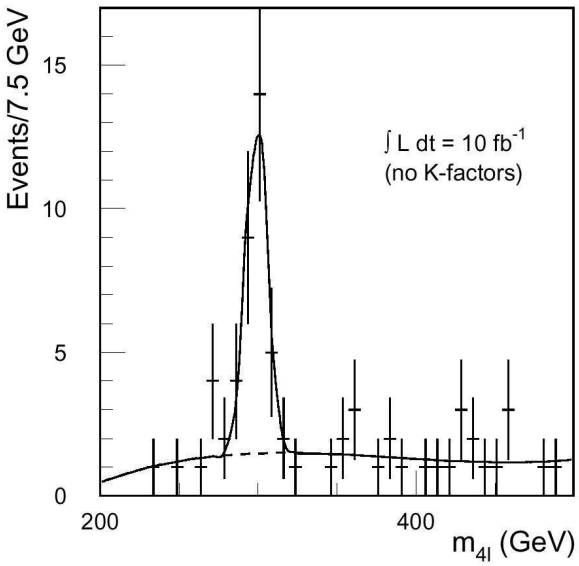

Fig. 4. *Invariant mass distribution for a 300 GeV Higgs signal over background in the four-lepton final state plotted for an integrated luminosity of 10 fb^{-1}.*

(depending on M_H) in a four-muon final state along. With additional $e^+e^-e^+e^-$ and $e^+e^-\mu^+\mu^-$ final states, number of signal events increases by a factor of four.

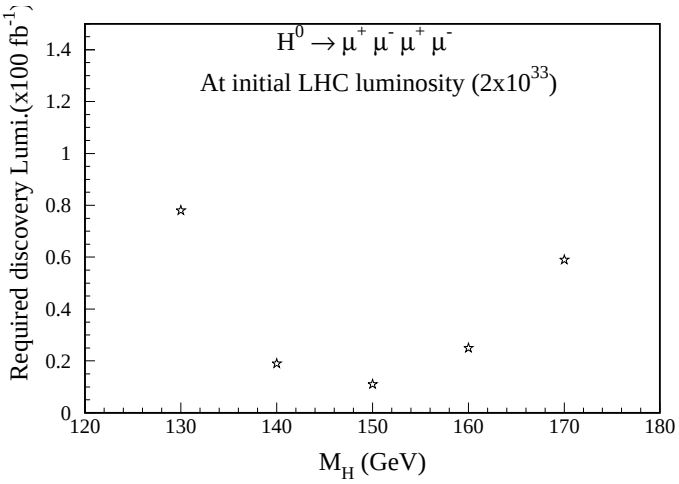

Fig. 5. *The required integrated luminosity as a function of the M_H to discover a Higgs boson of intermediate mass in the four-muon final state with a stand-alone ATLAS muon spectrometer.*

When the Higgs is lighter than about 130 GeV, it is difficult to discover it with low luminosity in the $H \to ZZ^* \to \ell^+\ell^-\ell^+\ell^-$ channel. The Higgs will be searched for through its decays $H \to \gamma\gamma$ and the associated production channel of $t\bar{t}H$. Higher integrated luminosities would be necessary in this case. The signal significances with the ATLAS detector for those channels are presented in Figs. 6 and 7. Searches in those channels are very challenging because of very large backgrounds. With conservative analysis approaches, using simple event selection cuts only and not using K-factors (higher order corrections, range of 1.1 - 1.9) in the calculations, the signal significance could reach 2.8σ-4.3σ in the $\gamma\gamma$ channel, and 5σ in the $t\bar{t}H$ channel for 100 fb^{-1} integrated luminosity.

Figure 8 shows the 160 GeV Higgs signals (in terms of accepted cross sections) from the decay mode of $H \to WW^* \to \ell\nu\ell\nu$ and sum of all the backgrounds in transverse mass (M_T) distributions.

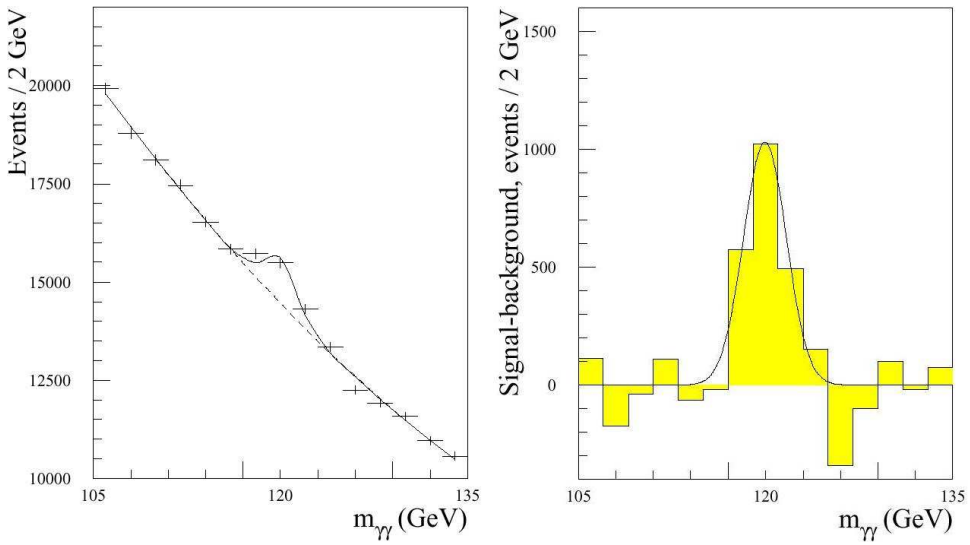

Fig. 6. *The left plot: Two-photon mass distribution for $H \to \gamma\gamma$ over sum of all backgrounds for an integrated luminosity of 100 fb^{-1}; the right plot is a background-subtracted two-photon spectrum to show a 120 GeV Higgs mass peak.*

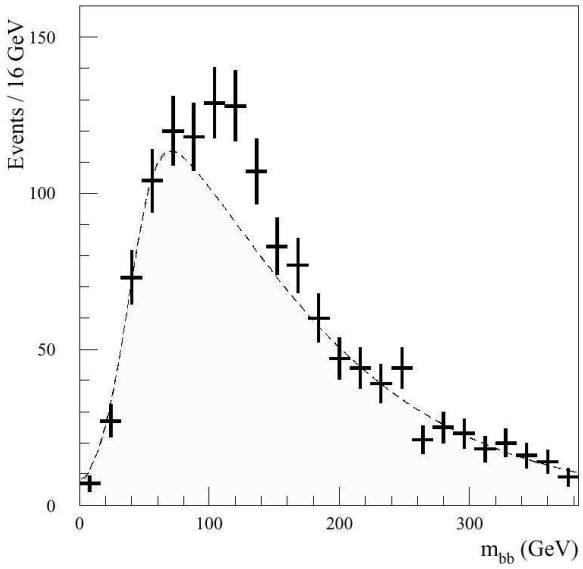

Fig. 7. *A 120 GeV Higgs signal (5σ) in two b-jet mass distribution over sum of all backgrounds (smooth curve) for an integrated luminosity of 100 fb^{-1}. Plotted signal is from the $t\bar{t}H$ channel with the Higgs decaying into the $b\bar{b}$, and at least one top quark decaying into an $\ell\nu + b$ final state.*

For a heavy Higgs ($M_H > 2M_Z$) the search will be relatively easy through the $H \to ZZ$ decay mode in final states of $\ell^+\ell^-\ell^+\ell^-$, $\ell^+\ell^+\nu\nu$ and $\ell^+\ell^- + jet\ jet$.

As shown in Figure 9, the complete analysis reported in the ATLAS Physics TDR demonstrates that the ATLAS experiment could discover the SM Higgs with combined signals in the first year of running of the LHC for an integrated luminosity of 30 fb^{-1}. One can see that at least two channels can be used for discoveries for the entire range of the Higgs mass.

Recent new results obtained by including the WBF channels in the study show that the signal significance has been further boosted in the low-mass region as shown in Figure 10.

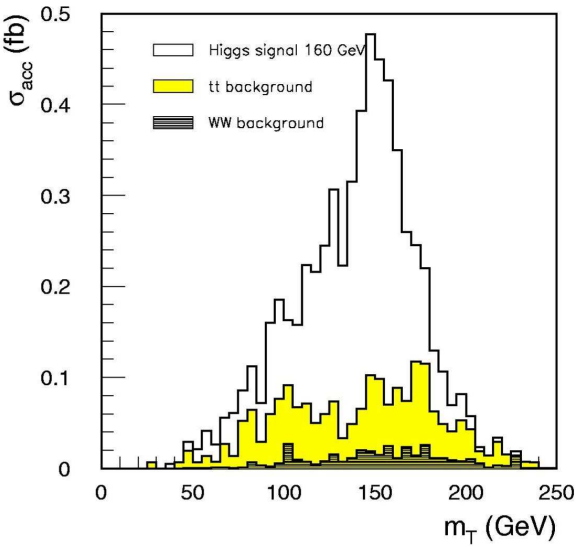

Fig. 8. *Transverse mass (M_T) distribution of a 160 GeV Higgs signals (in terms of accepted cross sections) for $H \to WW^* \to \ell\nu\ell\nu$ and sum of all the accepted backgrounds.*

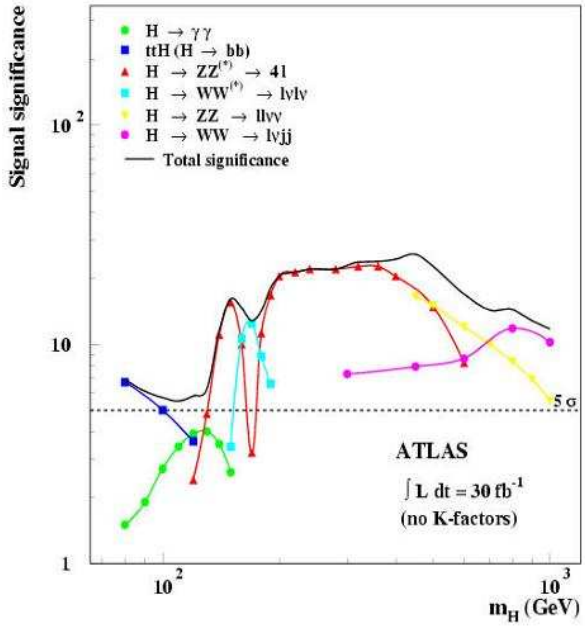

Fig. 9. *Higgs signal significance as a function of Higgs mass for an integrated luminosity of 30 fb^{-1}.*

2.2 Measurement of the Higgs Parameters at High Luminosities

Although we can discover Higgs boson with an integrated luminosity of 10 fb^{-1}, a high luminosity run will be very important to measure the Higgs parameters, as well as to study rare decay modes. The ATLAS potential for precision measurement of the Higgs parameters (mass, width, branching ratios, and couplings) should provide deep insight into the Higgs sector of the Standard Model and provide links to new physics beyond the SM.

The ultimate experimental precision with which ATLAS should be able to measure the Higgs mass is

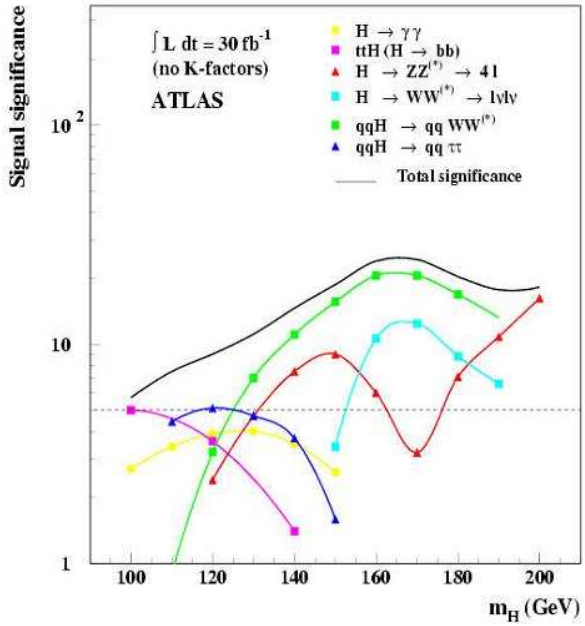

Fig. 10. *Higgs signal significance at the low-mass region for an integrated luminosity of 30 fb^{-1}. This plot includes the WBF channel in the studies, which significantly increases the sensitivity of the Higgs search in the low-mass region.*

shown in Figure 11. The precision can reach 0.1% for detections of leptonic and photon final states, and 1% for $b\bar{b}$ final state.

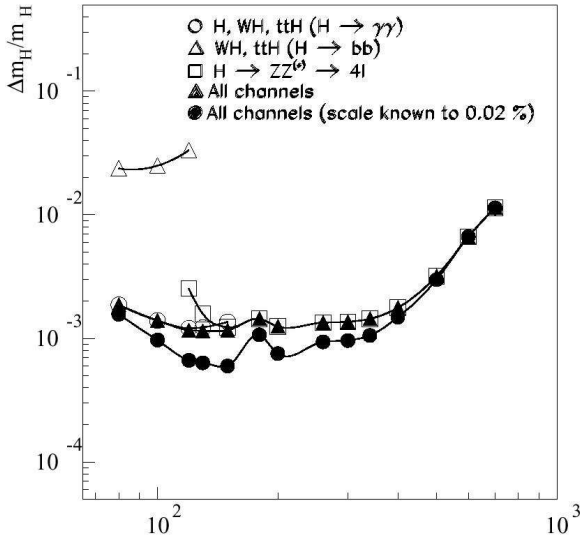

Fig. 11. *Measurements of the Higgs mass for an integrated luminosity of 300 fb^{-1}.*

We present the most recent study results for Higgs-coupling measurements with a global fit method [8] using all the production modes and detection channels. Figure 12 shows the expected accuracy of determination of branching fractions for the various decay modes as a function of Higgs boson mass with an integrated luminosity of 300 fb^{-1}. Branching fraction of $H \to ZZ$ can be determined with an accuracy of 10-20% if

Higgs is heavier than 125 GeV. It will be difficult to determine the branching fraction for the $b\bar{b}$ mode due to large background. The accuracy is about 50% for M_H =120 GeV. Figure 13 shows the expected accuracy of determination of Higgs couplings to various particles as a function of Higgs boson mass. We can determine the couplings of Higgs boson to Z, W, τ and top-quark with accuracies better than 20% if Higgs is heavier than 150 GeV.

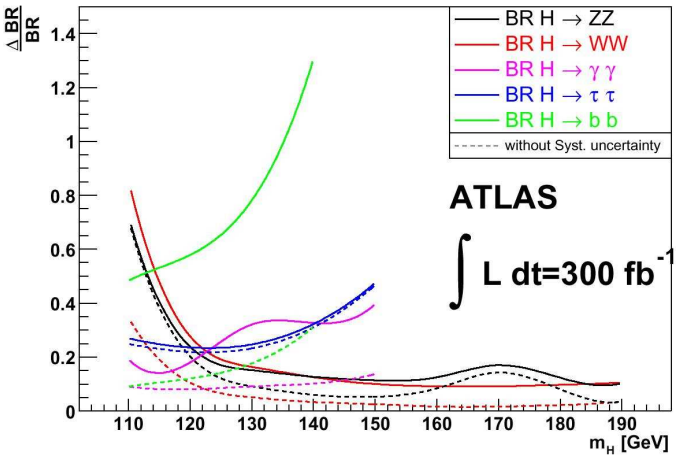

Fig. 12. *Measurements of the branching ratio of the Higgs decay modes for an integrated luminosity of 300 fb^{-1}.*

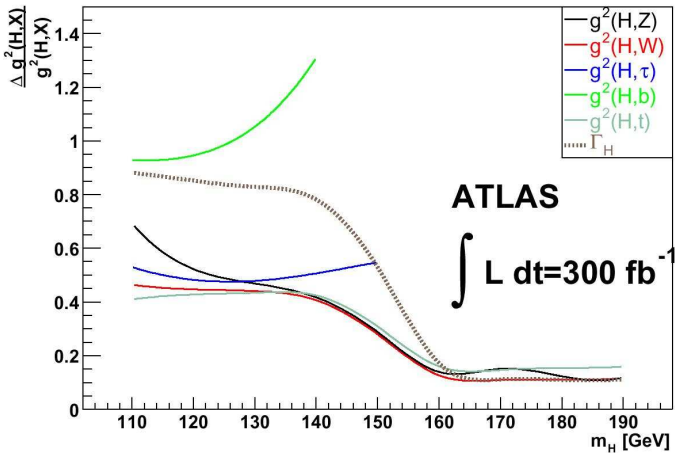

Fig. 13. *Measurements of the Higgs couplings for an integrated luminosity of 300 fb^{-1}.*

2.3 Higgs Self-Coupling and Rare Decay Modes at SLHC

A complete determination of the parameters of the Standard Model requires the measurements of the Higgs self-couplings. These include trilinear and quartic couplings:

$$\lambda^{SM}_{HHH} = 3\frac{m_H^2}{v}, \quad \lambda^{SM}_{HHHH} = 3\frac{m_H^2}{v^2}$$

where v is the vacuum expectation value. A direct measurement of λ_{HHH} can be obtained via the detection of Higgs pair production, where a contribution is expected from production of a single off-shell Higgs which decays into a pair of Higgs. However, production cross-section of this process is small and it is difficult to find the signals with a luminosity of $10^{34} cm^{-2} s^{-1}$. The measurements become accessible at the Super-LHC

M_H (GeV)	Signal	Background	Significance ($S/\sqrt{B}$)
170	350	4200	5.4
200	220	3352	3.8

Table 2. Signal significance of the Higgs self-coupling in the process of $gg \to HH \to 4W \to \ell^+\ell'^+4j$ for 6000 fb^{-1}.

Decay mode	cross section	$\int Ldt$	Significance
$H \to Z\gamma \to \ell\ell\gamma$	$\sim 2.5fb$	600 fb^{-1}	3.5
		6000 fb^{-1}	11
$H \to \mu\mu$	$Br \sim 10^{-4}$	6000 fb^{-1}	7.9*

Table 3. Signal significance of two rare decay modes of the Higgs for 6000 fb^{-1} at the SLHC. (* for m_H=120 GeV.)

with very high luminosities. Complete study results can be found in report [5]. Here we only quote the results obtained by investigating the process:

$$gg \to HH \to W^+W^-W^+W^- \to \ell^\pm\nu jj\ell^\pm\nu jj.$$

The expected numbers of signal events and background events from $t\bar{t}$, $W^\pm Z$, $W^\pm W^+W^-$, $t\bar{t}W^\pm$ and $t\bar{t}t\bar{t}$ channels are shown in Table 2. The signal significance is expected to be 5.4 for M_H=170 GeV, and 3.8 for M_H=200 GeV for an integrated luminosity of 6000 fb^{-1}. This allows a measurement of λ_{HHH} with statistical errors of 19% and 25% for m_H = 170 GeV and 200 GeV, respectively.

Two examples of rare Higgs decay modes observable at the SLHC are presented in Table 3. Those decay modes allow additional precision measurements of Higgs-couplings to gauge bosons and to fermions.

2.4 MSSM Higgs Discovery Potential

The supersymmetry model is one of the promising extensions of the Standard Model (references are listed in [4]). The Higgs sector of the Minimal Supersymmetric Standard Model (MSSM) contains two charged ($H^\pm$) and three neutral ($h,\ H,\ A$) physical states. At the tree level, all Higgs-boson masses and couplings can be expressed in terms of only two parameters: M_A, the mass of the CP-odd boson, and $tan\beta$, the ratio of vacuum expectation values of the Higgs doublets. Our study was focused on the discovery potential of various decay modes accessible also in the case of the SM Higgs boson: $h \to \gamma\gamma$, $h \to b\bar{b}$, $h \to ZZ \to 4\ell$, and of modes strongly enhanced at large $tan\beta$: $h \to \mu^+\mu^-$, $h \to \tau^+\tau^-$. Much attention was given also to the MSSM-specific decay modes such as: $H \to hh$, $A \to Zh$, $H^\pm \to \tau\nu$. The conclusions drawn from these studies were that the complete region of parameter space, M_A=50 - 500 GeV and $tan\beta$=1 - 50, should be accessible for discovery of the Higgs boson by the ATLAS experiment with 10 fb^{-1} integrated luminosity. If SUSY particles are light enough, decays of Higgs bosons to SUSY particles are accessible. The SM decay modes are then suppressed, competing in most cases with decays to charginos and neutralinos such as $H/A \to \chi_0^2\chi_0^2 \to 4\ell + missing - energy$. Detailed studies for the complex MSSM Higgs searches can be found in the ATLAS Physics TDR. We show an example of a signal from the process of $A/H \to \mu^+\mu^-$ observable with the ATLAS muon spectrometer in Figure 14. This channel has increased branching ratio for large $tan\beta$ comparing with the SM Higgs since the coupling of H/A to down type fermions are significantly enhanced. Thus, this channel is important not only for discoveries, but also for MSSM parameter $tan\beta$ determination with high luminosities as shown in Figure 15.

The 5σ-discovery contours in the M_A vs. $tan\beta$ parameter space for the MSSM Higgs searches with the ATLAS experiment are shown in Figure 16. Over a large fraction of this parameter space, more than one Higgs boson and/or more than one decay mode would be detectable. In the region of large m_A only the lightest Higgs boson h can be observed, unless the heavier Higgs bosons ($H,\ A,\ H^\pm$) have detectable decay

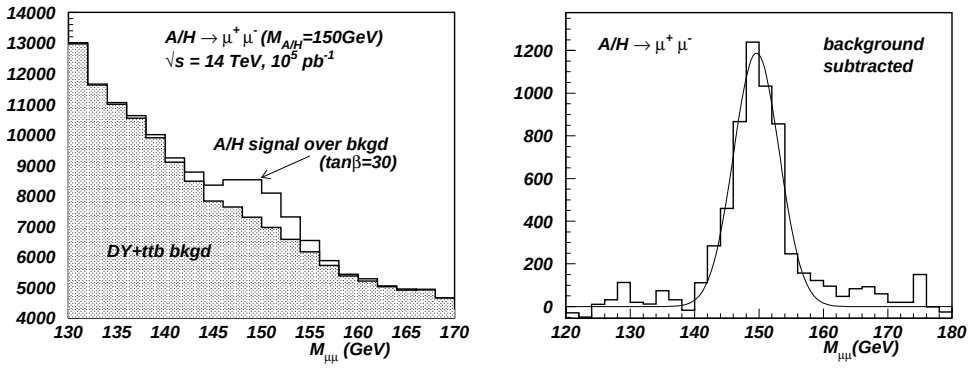

Fig. 14. *Di-muon invariant mass distribution for a 150 GeV MSSM Higgs decays: $A/H \to \mu^+\mu^-$. The left plot: Signal over the expected background; the right plot: background-subtracted signal. The plots are obtained for an integrated luminosity of 100 fb^{-1}.*

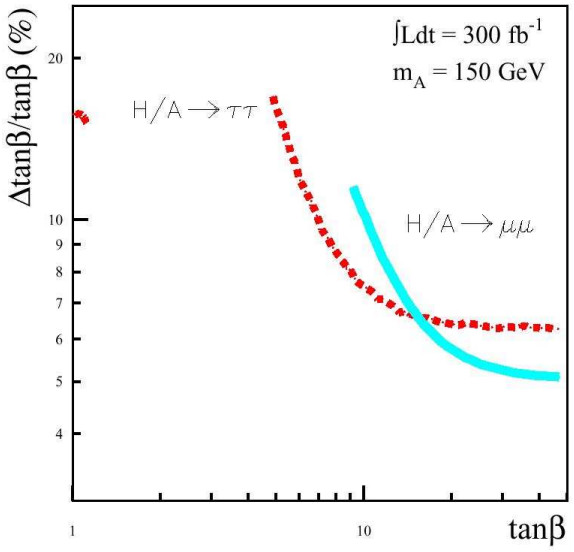

Fig. 15. *Determination of tanβ (M_A = 150 GeV) through the decay modes of $H/A \to \mu^+\mu^-$ and $H/A \to \tau^+\tau^-$. For an integrated luminosity of 300 fb^{-1}, the precision of the measurement can reach 5-15%.*

modes into SUSY particles. Our recent study show that the SLHC can extend significantly the discovery region over which at least one heavy Higgs boson can be discovered in addition to h, covering almost the full parameter space.

3 Strongly-coupled Vector Boson System

It may well be that no fundamental scalar particle exists. In this case, new physics must exist to account for the breaking of electroweak symmetry, for the regularization of the vector boson coupling, and for generating fermion masses. If no light Higgs boson is found, the study of electroweak symmetry breaking will require measurements of the production rate of energetic longitudinal gauge boson pairs since the longitudinal components are the Goldstone bosons of the symmetry breaking process. It will also be essential to search for the presence of new resonances that could regularize vector boson scattering cross-sections. Since the cross-section of these longitudinal resonances are small, high luminosity is necessary for clear signals. We show two examples of strongly-coupled resonances observable by the ATLAS detector at the SLHC in vector boson scattering processes in the TeV mass region with an integrated luminosity of 3000 fb^{-1}.

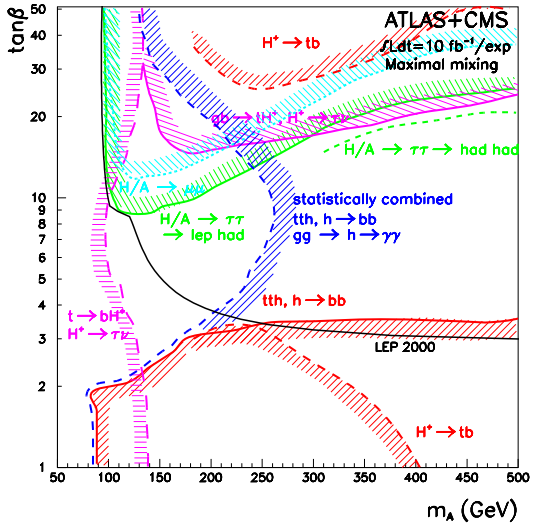

Fig. 16. *The 5σ-discovery contours in the M_A vs. tanβ parameter space for the MSSM Higgs searches.*

Figure 17 shows the resonance mass distribution in the W_LZ_L scattering process with a final state of three high-energy isolated leptons plus large missing transverse energy:

$$W_LZ_L \to W_LZ_L \to \ell\nu\ell\ell.$$

With an integrated luminosity of 300 fb^{-1}, the average number of detectable signal events would be 6.6 with an expected background of two events. With an order-of-magnitude luminosity increase at the SLHC, the signal significance ($S/\sqrt{B}$) becomes 10σ for 3000 fb^{-1}.

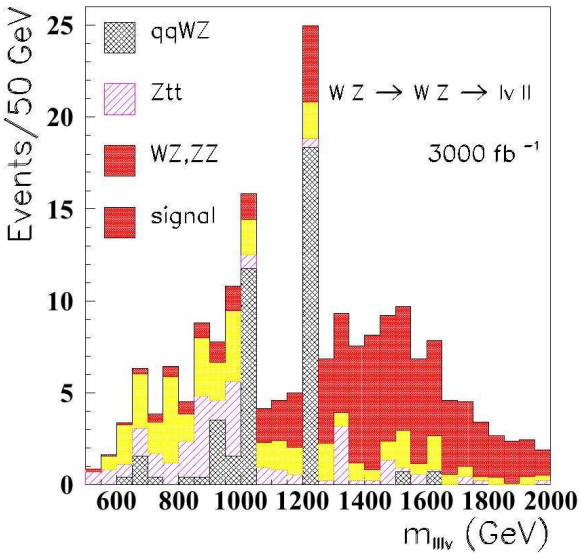

Fig. 17. *Expected signal and background for a 1.5 TeV WZ resonance in the leptonic decay channel for an integrated luminosity of 3000 fb^{-1}.*

Figure 18 shows the resonance mass distribution in the $Z_LZ_L(W_LW_L) \to Z_LZ_L$ scattering process with a final state of four high-energy isolated leptons.

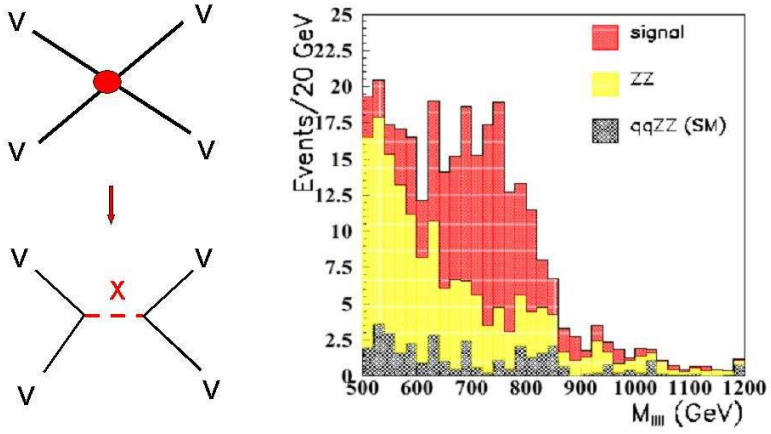

Fig. 18. *Diagram of four gauge boson scattering in the high energy regime (left). X in the diagram indicates new resonances which would be responsible for regularizing the vector boson scattering cross section. The right side histograms are the expected signal and background at the Super-LHC (for* $\int Ldt$ *=3000* fb^{-1}*) for a scalar resonance of mass 750 GeV decaying into four leptons.*

Final state	$jZ(\nu\nu)$	$jW(\tau\nu)$	$jW(e\nu)$	$jW(\mu\nu)$
Num. of events	523	151	12	14

Table 4. Expected background events in the $jets\ +\ missing\ E_t$ channel for 100 fb^{-1}.

Observations of the new resonances in the strongly-coupled vector boson system will certainly shine a bright light on the path to discover new physics beyond the SM.

4 Signals of Extra-Dimension Models

Assuming that a SM Higgs boson is discovered at the LHC, can we declare that all particle physics problems are solved? The answer would be "**NO**". The major unappealing characteristic of the SM is the so-called "hierarchy" problem in the gauge forces, with gravity being a factor of $10^{33}-10^{38}$ weaker than the other three. A new framework to solve the hierarchy problem was proposed recently [5], in which extra dimensions are introduced. In the presence of δ of these extra dimensions, the fundamental Planck scale in $4+\delta$ dimensions can be lowered to the TeV range, i.e., to a value comparable to the scale that characterizes the other three forces, thereby eliminating the puzzling hierarchy. Models of extra dimensions have recently raised much interest. They predict new phenomena in the TeV energy range, which can be tested at present and future colliders. Several models and signatures have been investigated and reported in [5]. We present below examples of the experimental signatures of direct or virtual production of gravitons, that can be detected by ATLAS at the LHC.

Figure 19 shows the direct graviton production signals from processes of $q\bar{q} \rightarrow gG,\ \gamma G$, $qg \rightarrow qG$, and $gg \rightarrow gG$, in $jets + missing\ E_t$ final state. The plot is obtained for $\int Ldt = 100\ fb^{-1}$. The events were selected by requiring jet energies larger than 1 TeV. The expected numbers of background events are listed in Table 4.

Significances are listed in Table 5 for various model parameters (δ: number of extra-dimensions, and M_D: gravity mass scale).

It has been found that the ATLAS reach in the gravity scale M_D for $\delta = 3$ increases from 7 TeV (100 fb^{-1} at LHC) to 11.7 TeV (3000 fb^{-1} at SLHC).

Figure 20 shows the experimental signatures in di-lepton mass distributions for virtual graviton exchange

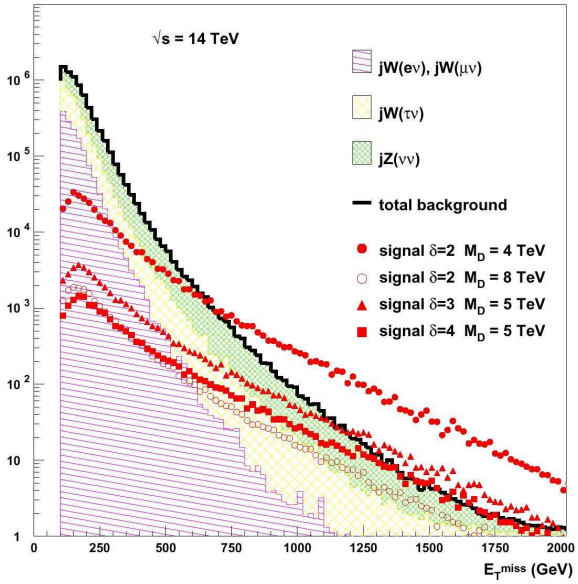

Fig. 19. *Missing transverse energy E_T^{miss} distribution for signals of the direct production of gravitons in large extra-dimension models, and expected background (histogram) for 100 fb^{-1} event-samples with jet energies larger than 1 TeV.*

δ	M_D (TeV)	Events	Significance
2	5	1430	61.4
	7	366	13.8
	9	135	5.1
3	5	705	26.7
	7	131	5.0
4	5	391	14.8
	7	53	2.0

Table 5. Expected numbers of signal events and significance in the *jets + missing E_t* channel for 100 fb^{-1}.

processes. Such signatures would show large enhancements in Drell-Yan di-lepton spectra. Clear signatures would also show up in forward-backward asymmetry (A_{FB}) measurements for di-lepton final states, which will require very clear charge identifications of the leptons. We show the excellent charge measurement of the ATLAS muon spectrometer in Figure 21. The fraction of multi-TeV muons with mis-identified charge is expected to be below 4% [7]. This capability will allow ATLAS to pin down different models once the new physics signals are observed as shown in Figure 22: the different parameters of the model are clearly distinguishable in the A_{FB} measurements.

Another interesting example of possible di-lepton physics, shown in Figure 23, is the resonance production in models of TeV^{-1} scale extra-dimensions. In this plot we have included resonances from different models. Again, the forward-backward asymmetry measurements will help to distinguish these models if a resonance is observed. Our detailed studies conclude that with 100 fb^{-1} integrated luminosity ATLAS can reach a mass scale up to ∼6 TeV.

Many models of extra-dimensions have been considered at the SLHC for an integrated luminosity of 3000 fb^{-1} [5]. These studies conclude that the ATLAS sensitivity in this case is of order 15-20 TeV.

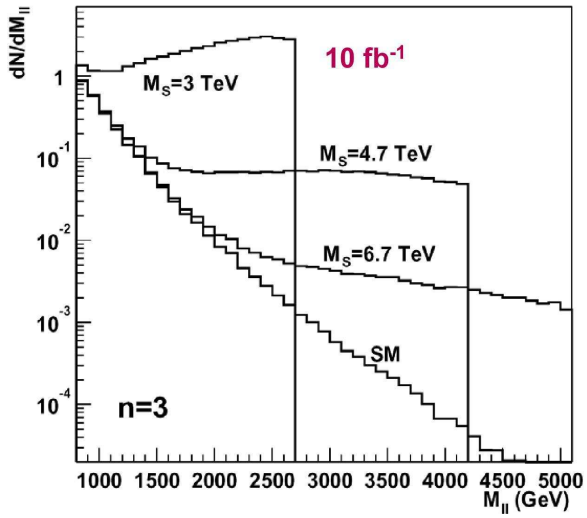

Fig. 20. *Expected signals from virtual production gravitons with different masses in di-lepton mass distribution for an integrated luminosity of 100 fb^{-1}. The SM Drell-Yan spectrum is shown together in the plot.*

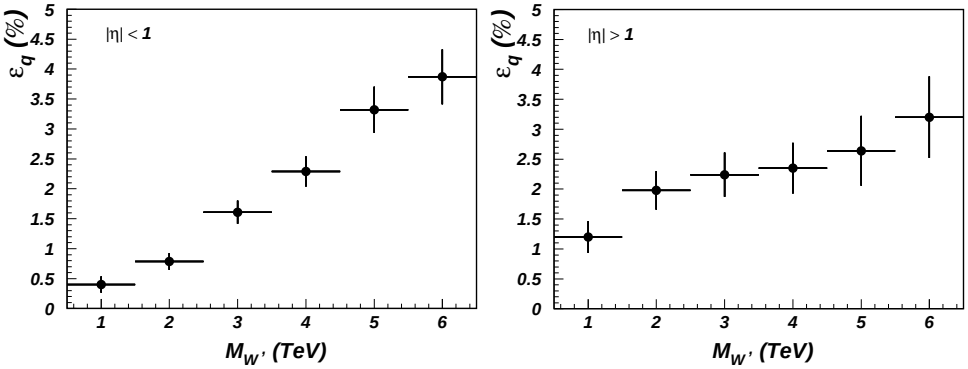

Fig. 21. *The fraction of muons with mis-identified charge in the ATLAS muon spectrometer in multi-TeV W' (new gauge boson) events. Barrel (endcap) fractions are shown in left (right) plot.*

5 Signals of Strong Symmetry Breaking

Technicolor models [9] are possible alternatives to the SM Higgs sector. Introduced by Weinberg and Susskind in 1979, they provide a dynamical means of breaking electroweak symmetry. These models introduce a new QCD-like force and new particles (techniquarks and technileptons), which can break electroweak symmetry and generate the vector boson masses without introducing fundamental scalars. Along with some necessary extensions to the theory, technicolor provides the known fermion masses, and it also predicts many new "techni-mesons." Many Technicolor discovery channels have been investigated by the ATLAS collaboration. These processes are shown in Figure 24.

The main backgrounds for signals of technihadron resonances are from $Z + jet$, $t\bar{t}$ and WZ events. We show the cleanest channel for detection of a technirho, ρ_T, in the following process:

$$\rho_T^{\pm} \to W^{\pm} Z \to \ell^+ \nu \ell^+ \ell^- .$$

Figure 25 presents the expected possible signal mass peaks and background.

Many other examples of detection of Technicolor signals with the ATLAS detector are reported in the ATLAS Physics TDR. Those studies show that ATLAS will be sensitive to the new resonances predicted in

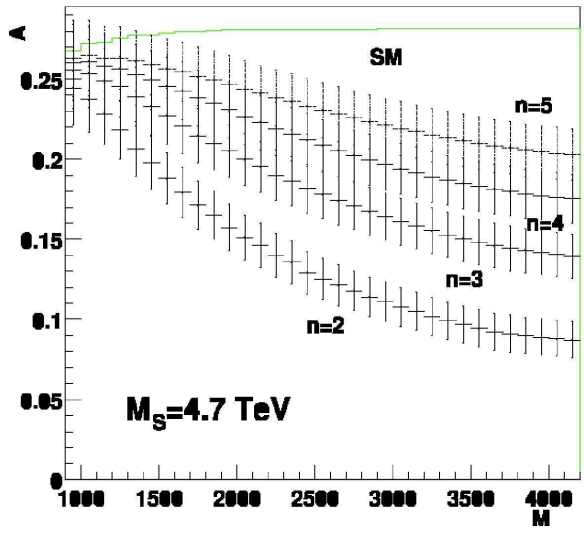

Fig. 22. *Forward-backward asymmetry measurement as a function of the di-lepton mass for different parameters in large extra-dimensions models. The new physics signals are clearly distinguishable from the SM prediction that is also shown in the plot.*

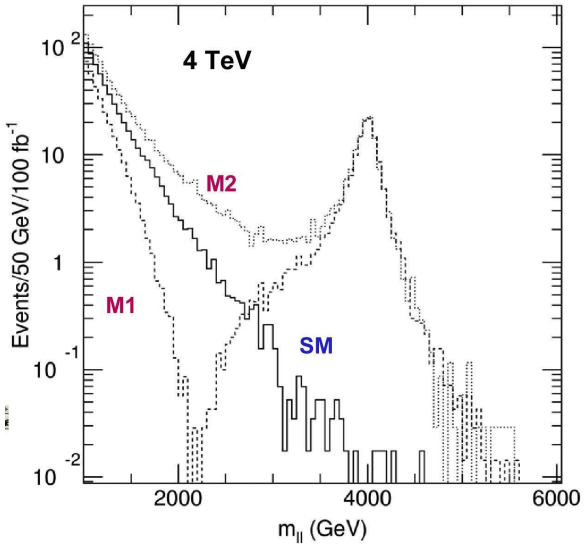

Fig. 23. *Resonance detection in the di-lepton mass spectrum using the ATLAS detector. Signals shown in the plots were obtained with an integrated luminosity of 100 fb^{-1}.*

the Techcolor theory, up to the TeV range at the LHC.

6 High-Precision Measurements at the SLHC

The high-precision studies performed at LEP have clearly indicated the essential role played by precision determinations of the electroweak parameters as a tool to search for the first signs of the inevitable breakdown of the Standard Model.

Study of multiple gauge boson production will provide an important test of the high energy behaviour of weak interactions. The cleanest final states are those where all W's and Z's decay leptonically, but these are compromised by small branching ratios. As a result, luminosity limits the number of possible channels

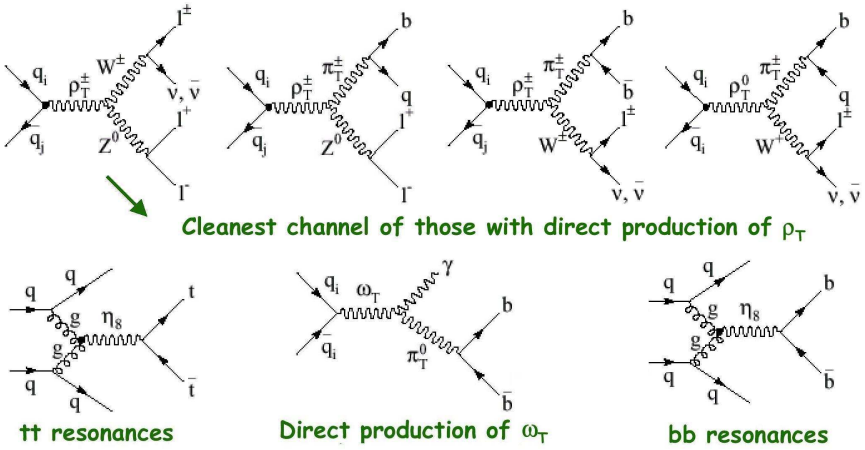

Fig. 24. *Feynman diagrams of the Technicolor discovery channels investigated by the ATLAS collaboration.*

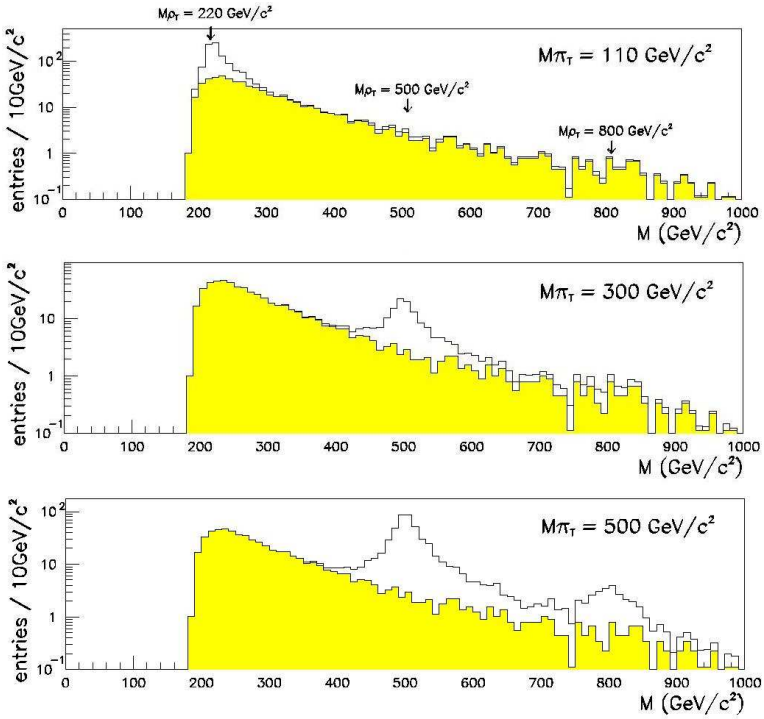

Fig. 25. $\rho_T^{\pm} \to W^{\pm}Z \to \ell^+\nu\ell^+\ell^-$*: reconstructed* $W^{\pm}Z$ *invariant mass spectrum for 30* fb^{-1}*. The solid line is for the* ρ_T *signal and the filled area for the* WZ *background. The three diagrams show the different parameters of* ρ_T *in the model.*

accessible at the LHC. With very high luminosities at the SLHC, the expected multiple gauge boson events become accessible (see Table 6) for high precision triple and quartic gauge boson coupling measurements.

6.1 Triple Gauge-Boson Couplings

In the SM, the triple gauge-boson couplings (TGC's) are uniquely fixed by gauge invariance and renormalizability. Extensions to the SM, in which for example the gauge bosons are not elementary but are bound states of more fundamental particles, generically lead to deviations from the SM prediction for the TGCs. The larger the available statistics, the higher the sensitivity to these deviations. In the case of a positive

Process	WWW	WWZ	ZZW	ZZZ	WWWW	WWWZ
N_1	2600	1100	36	7	5	0.8
N_2	7100	2000	130	33	20	1.6

Table 6. Expected numbers of multiple gauge boson events, N_1 for m_H=120 GeV, and N_2 for m_H=200 GeV, selected in pure leptonic final states for 6000 fb^{-1}.

indication of non-SM TGC's at the LHC, increased statistics at the SLHC should allow a deeper understanding of which specific realization of new physics is responsible for these deviations. The latter are in fact parameterized by effective interactions which, in order to preserve unitarity at high energy, require the inclusion of form factors. The mass scale Λ which is needed to define such formfactors is typically associated with the scale at which new physics manifests itself. A measurement of the energy dependence of the TGC's will probe the shape of the form factor, and therefore allow extraction of the value of the scale Λ.

Assuming electromagnetic gauge invariance and C- and P-conservation, five parameters can be used to describe the triple-gauge vertices: g_1^Z, $\Delta\kappa_\gamma$, $\Delta\kappa_Z$, λ_γ, and λ_Z.The SM values of these parameters, at tree level, are one for g_1^Z and zero for the others.

At the LHC two processes can be studied to access these TGCs: $W\gamma \to \ell\nu\gamma$, which probes the couplings λ_γ and $\Delta\kappa_\gamma$, and $WZ \to \ell\nu\ell\ell$, which probes the couplings λ_Z, $\Delta\kappa_Z$ and g_1^Z.

ATLAS expected sensitivities to the TGCs for different luminosity scenarios are shown in Figure 26. It

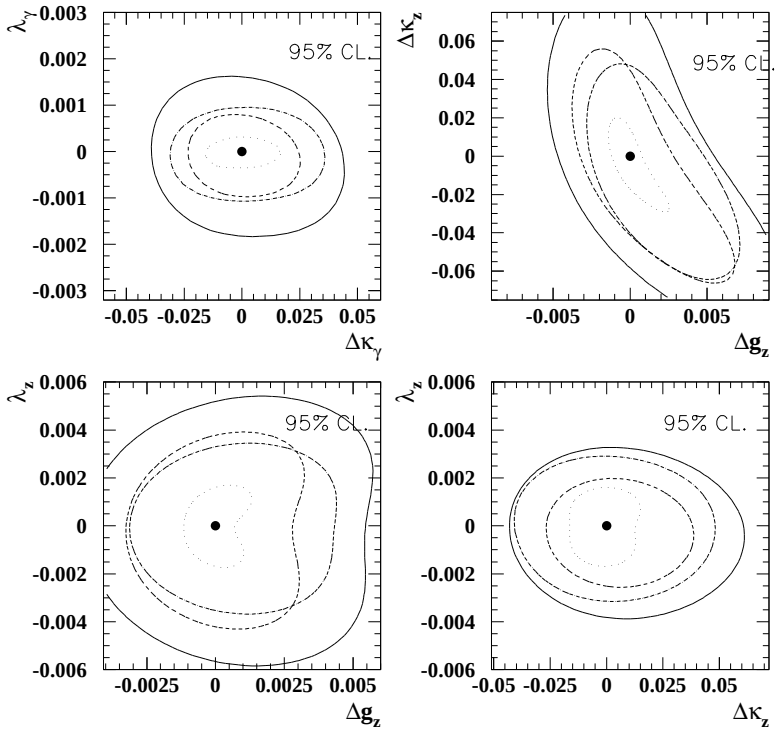

Fig. 26. *Expected 95% C.L. constrains on triple gauge couplings in ATLAS, resulting from two-parameter fits (Λ = 10 TeV). The contours correcpond to 14 TeV and 100 fb^{-1} (solid), 28 TeV and 100 fb^{-1} (dot dash), 14 TeV and 1000 fb^{-1} (dash) and 28 TeV and 1000 fb^{-1} (dotted).*

can be seen that a tenfold luminosity increase at the SLHC should extend the sensitivity for the λ-type and g_1^Z parameters into the range of $\sim 10^{-3}$ expected from the radiative corrections in the SM, and should therefore allow a meaningful test of these corrections and others that arise for example in supersymmetric

models.

6.2 Quartic Gauge-Boson Couplings

Similarly to the TGCs, quartic gauge-boson couplings (QGC) are an essential component of the electroweak theory. As in the case of TGC's, possible deviations from the SM prediction are parameterized in terms of effective terms in the Lagrangian that lead to genuine quartic vertices (α_4, α_5, α_6, α_7, α_{10}).

Figure 27 shows the $1-\sigma$ contours and the correlations in the parameter space for W^+W^-, $W^\pm W^\pm$, $W^\pm Z$ and ZZ scattering processes at the LHC and the SLHC. Typical sensitivities of these parameters can attain the 10^{-3} level in the SLHC to allow a stringent test of the SM.

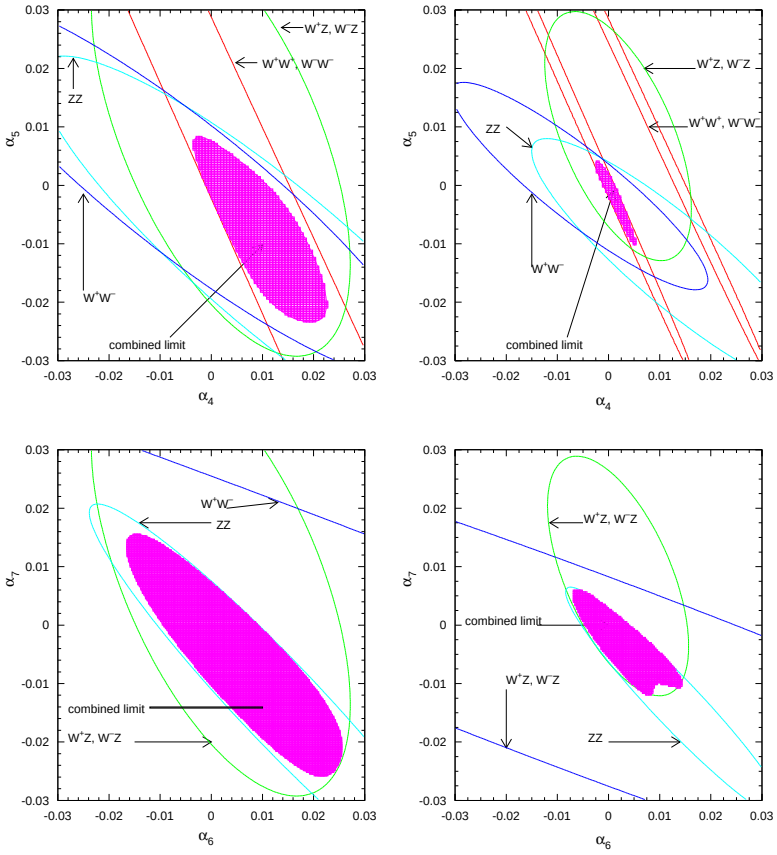

Fig. 27. *Top plots: 1-σ contours in the $\alpha_4-\alpha_5$ plane for W^+W^-, $W^\pm W^\pm$, $W^\pm Z$ and ZZ production for an integrated nominosity of 100 fb^{-1} (top, left) and 6000 fb^{-1} (top, right) with assumptions of $\alpha_6=\alpha_7=\alpha_{10}=0$.*
Bottom plots: 1-σ contours in the $\alpha_6-\alpha_7$ plane for W^+W^-, $W^\pm W^\pm$, $W^\pm Z$ and ZZ production for an integrated nominosity of 100 fb^{-1} (bottom, left) and 6000 fb^{-1} (bottom, right) with assumptions of $\alpha_4=\alpha_5=\alpha_{10}=0$.

7 Summary

We have presented some examples of the expected physics results at the LHC high and very high luminosities based on detail simulations of the ATLAS detector's response for a selection of electroweak, extra-dimension, and new strong-force physics processes. We have also show the capability of ATLAS to perform high precision measurements of the electroweak parameters to search for a breakdown of the Standard Model.

We summarize our principal conclusions:

- The SM and the MSSM higgs bosons could be discovered in the first year physics program of the LHC with a total integrated luminosity of 10 - 30 fb^{-1}.
- Measurements of the Higgs parameters can reach a precision of 0.1-1.0% in mass determinations; 5-30% in branching-ratio determinations; and 10-40% in the couplings with a total integrated luminosity of 300 fb^{-1}.
- Rare SM Higgs decay modes, such as $H \to Z\gamma$ and $H \to \mu^+\mu^-$, and Higgs self-interactions can be observed with more than 5σ significance for 3000 fb^{-1} at the Super-LHC.
- If no Higgs is found, resonance and non-resonance scattering of gauge bosons at TeV energies could be fully explored with a signal significance great than 10σ for 3000 fb^{-1}.
- The mass reach for extra-dimension models will be extended up to an order of 10 TeV at high luminosities of the LHC.
- Measurements of triple and quartic gauge-boson couplings can be improved significantly over LEP and Tevatron results at the Super-LHC to allow very stringent tests of the Standard Model.

We have not discussed important searches for the supersymmetric particles in this paper. A detailed discussion and the SUSY particle mass reach of the ATLAS experiment can be found in the ATLAS Physics TDR. Many other interesting topics of new physics which are not presented in this paper, such as leptoquarks, compositeness, black holes, and monopoles, will also be explored by ATLAS. More importantly, we will be exploring the **unknown** at the LHC.

8 Acknowledgment

The author would like to thank Fabiola Gianotti and Frank Taylor for their detailed comments and suggestions to the topics presented. A special thank to Rudi Thun for his proof-reading of the manuscript.

References

1. ATLAS Technical Proposal for a General Purpose pp Experiment at the Large Hadron Collider at CERN, The ATLAS Collaboration, (CERN/LHCC/94-43).
2. “GEANT3,” R. Brun et al. (CERN/DD/EE/84-1).
3. “ATLFAST: A package for particle-level analysis,” E. Richter-Was et al. (ATL-PHY-079).
4. ATLAS Detector and Physics Performance TDR, The ATLAS Collaboration (CERN/LHCC/99-14).
5. “Physics Potential and Experimental Challenges of the LHC Luminosity Upgrade,” F. Gianotti et al. (CERN-TH/2002-078).
6. “Detection Sensitivity for Intermediate Mass Higgs through Muon Final State with ATLAS Detector,” Shank, J ; Sliwa, K ; Taylor, F ; Zhou, B ; (ATL-MUON-97-206).
7. ATLAS Muon TDR, The ATLAS Muon Collaboration (CERN/LHCC/99-15).
8. “Measurement of Higgs-couplings,” by M. Duehrssen (http://agenda.cern.ch/fullAgenda.php?ida=a0376)
9. “Technicolor Signatures - Ieri, Oggi Domani,” K. Lane, (hep-ph/0006134).